










High accuracy dual split ring resonator-defected ground structure based microwave sensor for material characterization

Mohamad Harris Misran^{1,*} , Maizatul Alice Meor Said¹ ,
Mohd Azlishah Othman¹ , Siti Normi Zabri¹ , Eliyana Ruslan¹ ,
Noor Azwan Shairi¹ , Zahriladha Zakaria¹ , Suleiman Aliyu Babale² ,
Mohd Zahid Idris³ 

¹Centre for Telecommunication Research & Innovation (CeTRI), Fakulti Teknologi dan Kejuruteraan Elektronik dan Komputer (FTKEK), Universiti Teknikal Malaysia Melaka (UTeM), Hang Tuah Jaya, 76100, Durian Tunggal, Melaka, Malaysia.

²Department of Electronics and Telecommunications Engineering, Ahmadu Bello University, Zaria, Kaduna State, Nigeria.

³Marine Engineering and ETO, Abu Dhabi Maritime Academy, 6th Street, Musaffah M-14, Abu Dhabi, United Arab Emirates.

*Corresponding author: harris@utem.edu.my

Original Research

Received:
7 May 2025
Revised:
17 July 2025
Accepted:
3 August 2025
Published online:
3 September 2025
Published in issue:
25 September 2025

© 2025 The Author(s). Published by the OICC Press under the terms of the [Creative Commons Attribution License](#), which permits use, distribution and reproduction in any medium, provided the original work is properly cited.

Abstract:

Microwave sensors have grown in popularity in recent years because of their contactless sensing capability, real-time detection capability, measurement, accuracy, ease of manufacture and robustness. They have become one of the primary choices in smart sensing applications. However, some of their key limitations, such as accuracy, sensitivity, and selectivity, might be regarded as limiting their utilization and application range. Thus, this project proposed to design and develop a high-accuracy microwave sensor for material characterization. This microwave sensor uses a Defected Ground Structure (DGS) to enhance sensor accuracy in determining the dielectric characteristics of the material under test (MUT). The sensor achieved high accuracy with a percentage error of 0.56% to 1.86% for the tested various MUTs, demonstrating reliable precision. The DGS significantly enhances performance, optimizing efficiency and compactness while reducing transmission losses on cost-effective substrates like FR4. Its high Q-factor of 595 enables detecting small dielectric constant variation.

Keywords: Microwave sensor; Defected ground structure; High accuracy; Split ring resonator

1. Introduction

A substance's permittivity controls how it responds to electromagnetic (EM) radiation. Therefore, for applications involving non-destructive testing, microwave circuit design, and antenna design, accurate permittivity measurement is crucial.

In recent years, microwave sensors have come to importance as one of the trending topics in theory and design and are progressively being used in a variety of modern microwave

systems [1]. To maintain sensor fabrication simplicity, low cost, and integration with planar circuits, the microstrip technique has been used for fabrication [2]. Furthermore, a major advantage of the sensor is their ease of placement on a circuit board. Microstrip patches are inexpensive and easy to construct [3].

Previous designs of microwave sensors have made significant strides in addressing the inherent challenges of sensitivity, accuracy, and reliability in permittivity characterization. For instance, designs incorporating interdigital capacitors

(IDC) have been highly effective in enhancing electromagnetic field confinement, resulting in improved interaction between the sensing field and the MUT [4].

Additionally, complementary split-ring resonators (CSRR) have been integrated into sensor designs to enhance sensitivity and selectivity, particularly for substrates with varying dielectric properties. These sensors have shown significant improvements, with sensitivity reaching 35.07 MHz/unit permittivity, while maintaining a compact form factor suitable for miniaturized applications [5]. Other designs have employed interdigital capacitors combined with dual-gap split-ring resonators to generate high-intensity coupled electric fields, improving sensor sensitivity [6].

In addition, planar microwave sensors utilizing advanced structural optimizations have proven effective for simultaneous characterization of permittivity and permeability. These designs focus on generating high-intensity electric and magnetic field zones, achieving dual-resonance capabilities while maintaining compactness and high resolution [7].

These innovative approaches in microwave sensor design have established a strong foundation for addressing challenges related to signal loss, miniaturization, and performance in real-world applications, thereby paving the way for reliable and precise permittivity characterization. The split ring resonators (SRR) and CSRR structures are commonly used in planar resonators among permittivity characterization methods [8].

2. Methodology

Microwave sensors have various types of shapes. Before designing, the shape of the antenna should be determined.

Square, circular and hexagonal sensors were simulated and analyzed. In this project, the rectangular shape has been chosen as the final design due to its lowest return loss compared to the circle and hexagon shapes as shown in Fig. 1. As shown in Fig. 1, the square antenna generally outperforms circular and hexagonal antennas in terms of S_{11} due to its better impedance matching, stable current distribution, controlled bandwidth, and easier fabrication, resulting in lower reflection loss and improved efficiency. The square shape provides sharp edges and corners, which enhance the electric field confinement and reduce reflection, leading to lower return loss, S_{11} . Additionally, the square geometry offers greater design flexibility, allowing for easier optimization of the resonant frequency and bandwidth. In contrast, circular and hexagonal designs tend to have more gradual field transitions, which can result in higher reflections and reduced efficiency, thus negatively impacting their S_{11} performance.

To increase the Q factor and lower S_{11} , an inset feed technique was introduced, as illustrated in Fig. 2. This method improves impedance matching by adjusting the feeding position closer to the resonant point, which minimises reflection and enhances the efficiency of power transfer. Performance optimisation is further achieved by carefully tuning the size of the truncated patch and the inset feed depth. By varying these parameters through simulation and parametric analysis, the most suitable dimensions are identified to ensure optimal S_{11} performance, resonance stability, and efficient coupling with the sensor structure. This design approach enables precise control over input impedance, leading to improved overall sensor sensitivity and accuracy.

Fig. 3 illustrates the S_{11} performance of antennas with three

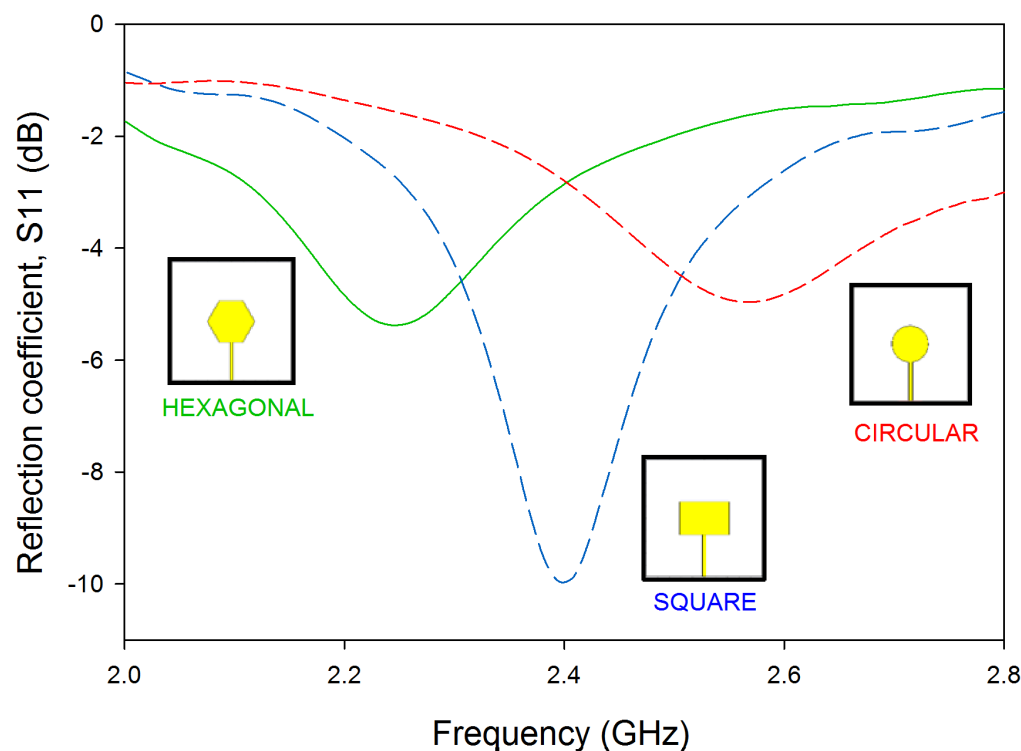


Figure 1. Performance comparison of three different antenna shapes.

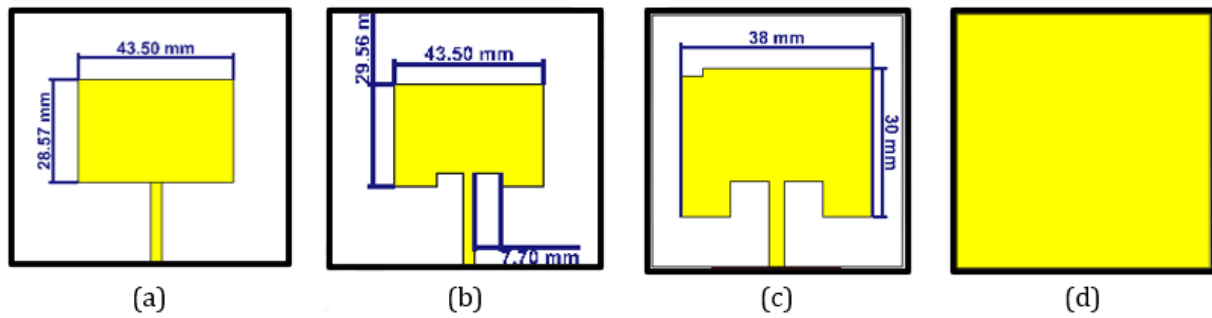


Figure 2. Microwave sensor (a) square patch (b) square patch + feed (c) square patch + truncated and (d) full ground plane for all design.

configurations: Square, inset-fed, and truncated designs. The square antenna exhibits a higher return loss, indicating less effective impedance matching at the resonant frequency. In contrast, the inset-fed and truncated designs achieve significantly improved return loss, with deeper nulls at approximately 2.4 GHz. This improvement demonstrates that these modifications enhance the antenna's impedance matching and reduce signal reflection. This leads to a stronger and more focused E-field in the vicinity of the feed point, reducing power loss and improving impedance matching. This adjustment narrows the bandwidth, focusing the sensor's response to a more specific frequency range.

The design process advanced with the implementation of a DGS to enhance antenna performance. Both single-ring and double-ring configurations were simulated and compared as shown in Fig. 4. The SRR is widely utilised in microwave sensors due to its high Q-factor, which enables sharp resonance peaks, enhancing sensitivity to material property variations. Its circular geometry supports strong current distribution and localized electromagnetic field confinement, improving interaction with the test material for precise sensing. The SRR is positioned at the center to max-

imize current distribution and electric field confinement, thereby enhancing the overall sensitivity of the system. Additionally, the SRR's dual electric and magnetic field coupling allows effective detection of dielectric and permeability changes, making it an optimal choice for compact, high-performance microwave sensors.

Referring to Fig. 5, DGS is implemented to enhance performance by improving S_{11} , leading to better impedance matching. This reduction in return loss indicates that the sensor is reflecting less energy and radiating more efficiently. The double-ring DGS demonstrated superior performance, achieving better impedance matching, deeper return loss values, showcasing its effectiveness over the single-ring configuration. Consequently, the Q factor increases significantly, indicating improved selectivity and sharper resonance, making the sensor more effective for precise applications.

A simulation was performed by placing the MUT on top of the sensor as illustrated in Fig. 6. During the simulation, the permittivity of the sensor was varied from 1 to 10, allowing the effect on the resonant frequency shift to be thoroughly analyzed as depicted in Fig. 7. This variation in permittivity helps in understanding how different dielectric

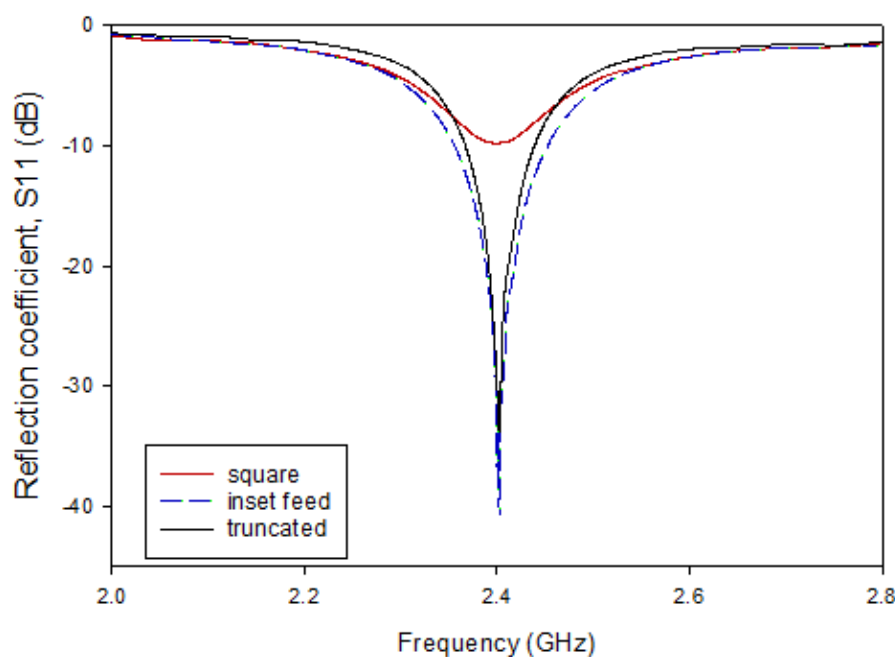


Figure 3. Simulation of square patch with inset feed and truncate implementation.

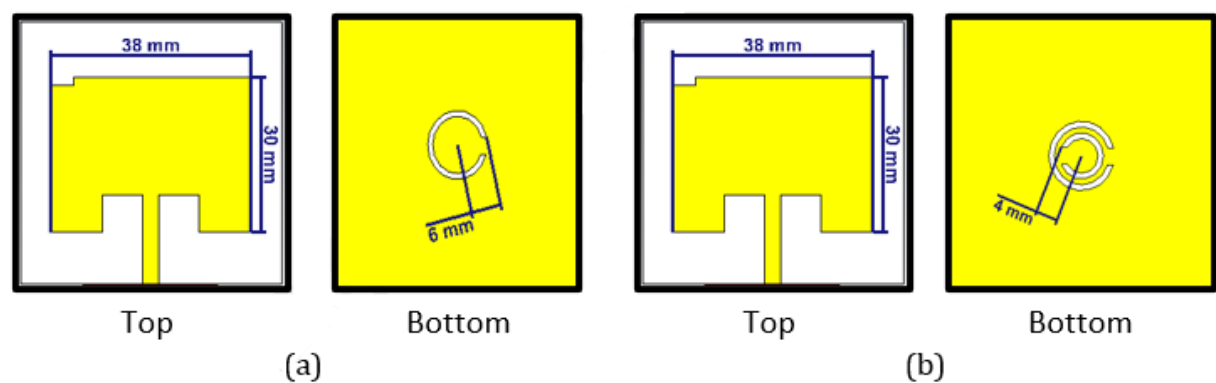


Figure 4. DGS implementation with (a) single SRR and (b) double SRR.

materials impact the sensor’s resonant behaviour. As the permittivity increases, the resonant frequency shifts lower, due to the sensor’s increased ability to store electric energy in the presence of the dielectric material. In microwave sensor characterization of solid MUTs using a VNA, small frequency shifts can make accurate dielectric constant extraction challenging. To minimize errors, simulations are performed for various MUT dielectric constants, and the resonant frequency is precisely read using markers on the VNA to avoid misinterpretation of S-parameters. A graph is plotted, and an equation is extracted, allowing dielectric constant determination directly from the measured reso-

nance frequency, reducing reliance on manual S-parameter readings and enhancing measurement reliability. The data collected from the simulation was then used to plot a graph of the shifted resonant frequency against the dielectric constant and loss tangent, as shown in Fig. 8 and Fig. 9, respectively. This graph provides an ideal case scenario, and comparing real-world measurements with this simulated reference graph, researchers can determine the dielectric properties of various materials with high precision. Second-order and third-order polynomial equation extracted from the simulation plotted graph using equation (1) and equation (2) to determine the measured MUTs’

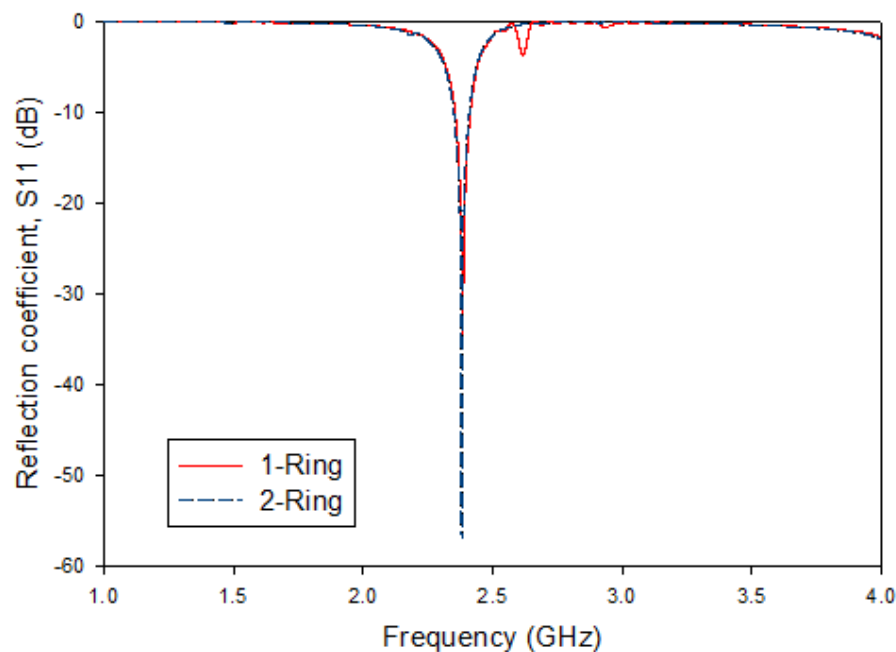


Figure 5. Simulation of rectangular patch with different number of rings.



Figure 6. MUT arrangement for material fabrication.

dielectric constant and loss tangent, respectively. The complete second-order and third-order polynomial equations are shown on the plotted graph as a reference equation for the sensor.

$$y = Ax^2 + Bx + C \quad (1)$$

$$y = Ax^3 + Bx^2 + Cx + D \quad (2)$$

The sensitivity and Q-factor of the sensor can be determined by using equation (3) and equation (4), respectively.

$$\text{Sensitivity, } S = \frac{\Delta f_{\text{shifted}}}{\Delta \epsilon_r} \quad (3)$$

[7]

$$Q \text{ factor} = \frac{2f_0}{BW}, \quad f_0 \text{ is center frequency} \quad (4)$$

[2]

The sensor was fabricated using an FR4 substrate, a widely used material in microwave and RF applications due to its cost-effectiveness and acceptable dielectric properties as shown in Fig. 10. Once the sensor was constructed, its S_{11} parameter was measured using a VNA in a controlled laboratory setup. This step is essential to ensure that the fabricated sensor's performance aligns with the simulation results, particularly in terms of resonant frequency and return loss. In

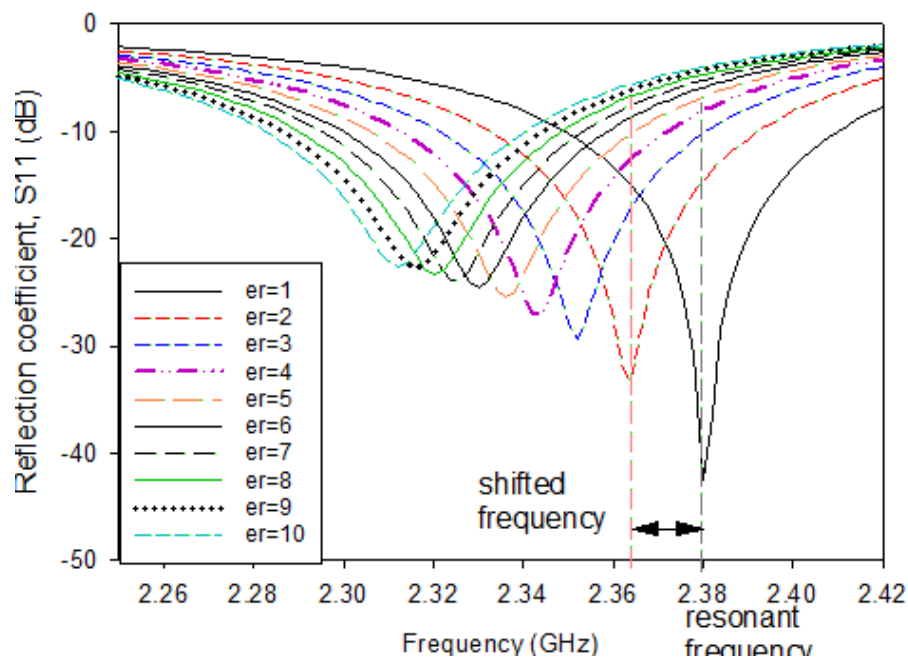


Figure 7. Frequency shifting with different dielectric constants, ϵ_r .

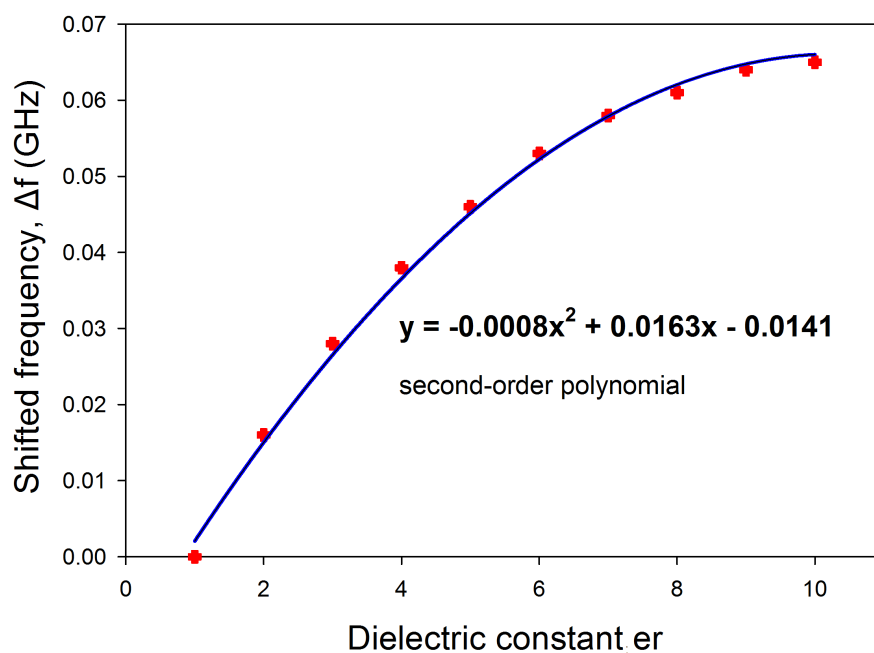


Figure 8. Second-order polynomial for MUT's permittivity.

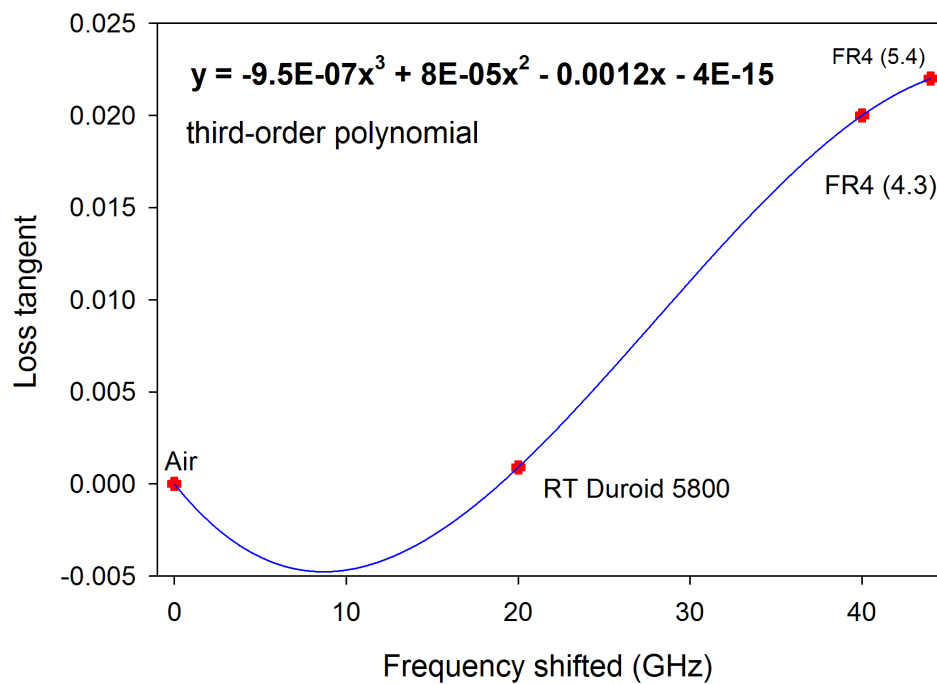


Figure 9. Third-order polynomial for MUT's permeability.

microwave sensors, noise can distort S-parameter measurements, reduce sensitivity to permittivity and permeability changes, and introduce instability in resonance frequency detection. As a solution, to enhance measurement accuracy, calibration techniques (e.g., Short-Open-Load-Thru, SOLT), low-noise cables and connectors to minimize signal degradation, EMI shielding to prevent external interference, and averaging techniques in the VNA to suppress random noise should be applied.

3. Results and discussion

The fabricated sensor was measured using a VNA to verify the accuracy of its performance compared to the simulation. In this study, three different MUT were evaluated: FR4 with a dielectric constant of 4.3, FR4 with a dielectric constant of 5.4, and RT Duroid 5880. These materials were placed on top of the sensor, and their respective S_{11} parameters

were measured.

Referring to Fig. 11, the measured S_{11} shows close agreement with the simulated results, with a slightly reduced return loss. This insignificant reduction could be attributed to radiation losses at the network's input or output ports due to imperfect connections. Moreover, fabrication quality plays a crucial role in achieving accurate sample characterization. Dimension imperfections and uncertainties introduced during the fabrication process can affect the sensor's response, particularly causing variations in the frequency shift.

The measured shifted resonance frequency data was utilized to calculate the dielectric constant of the MUT using a second-order polynomial equation. This approach ensures accurate characterization by fitting the frequency shift to the MUT's dielectric properties. Similarly, the loss tangent of the MUT was determined using a third-order polynomial equation, which provides a more precise estimation

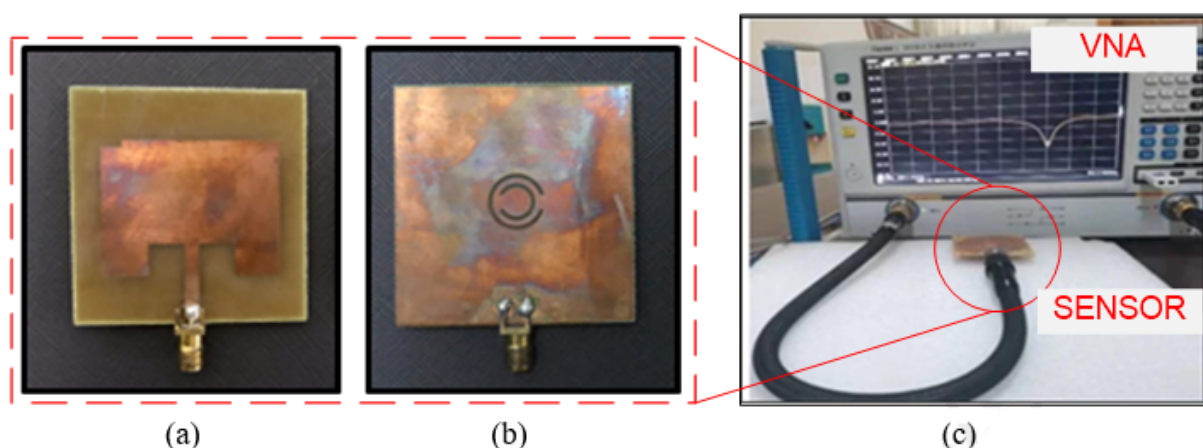


Figure 10. Fabricated sensor (a) top and (b) bottom view (c) with lab measurement setup.

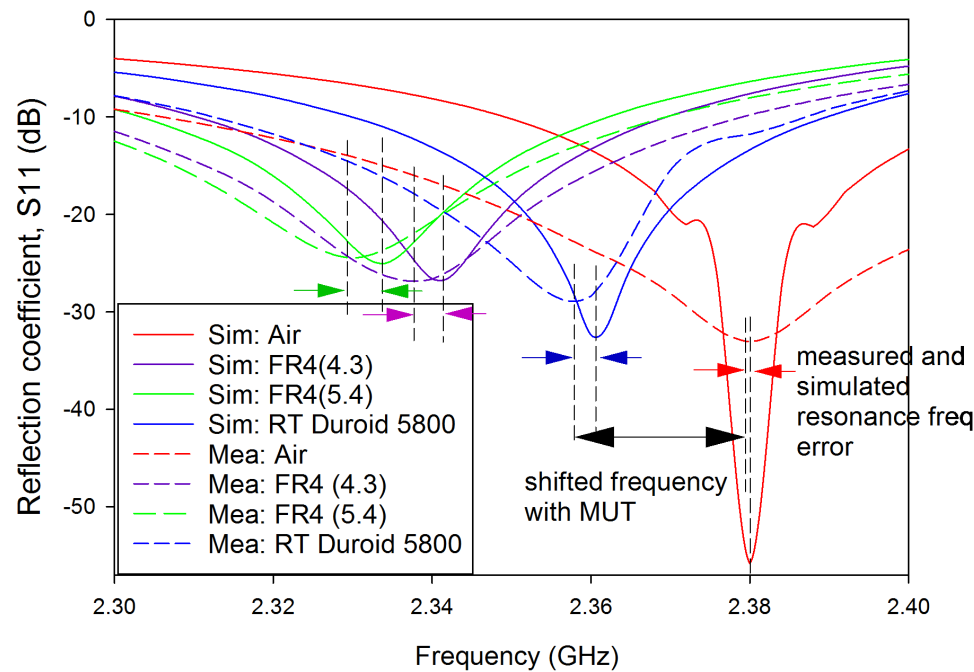


Figure 11. Comparison between measurements and simulations S_{11} .

of energy dissipation within the material. The use of these polynomial equations allows for higher accuracy in correlating frequency shifts and material properties. The summarized results in Table 1 highlight the calculated dielectric constants and loss tangents, showcasing consistency and reliability in the measurements.

Fig. 12 illustrates the comparison between the simulated and measured dielectric constant positions, highlighting the alignment and discrepancies between the two methods. This alignment ensures the credibility of the proposed sensor's ability to accurately characterize the dielectric constant of

materials accurately. The results indicate a close agreement between the measured and simulated dielectric constant values, with only negligible deviations. This consistency between the measured and simulated values highlights the sensor's high precision in material characterization. The percentage errors for the three samples which are FR4 (4.3), FR4 (5.4), and RT Duroid 5800 were 1.86%, 0.56%, and 1.46%, respectively. These results highlight the sensor's exceptional accuracy, with a measurement precision of more than 98% for both FR4 (4.3) and FR4 (5.4), and 99.74% for RT Duroid 5800. The measure loss tangent also

Table 1. Performance of the sensor.

		Air	FR4 (4.3)	FR4 (5.4)	RT Duroid 5800
Simulation (GHz)		2.38	2.340	2.334	2.360
Measurement (GHz)		2.381	2.340	2.332	2.363
Shifted Freq (MHz)		2	41	49	18
Dielectric Constant	Reference	1	4.3	5.4	2.2
	Measured	0.98	4.38	5.37	2.23
Accuracy (%)		98.00	98.14	99.44	98.64
Loss Tangent	Reference	0	0.0009	0.02	0.022
	Measured	0.00209	0.001	0.0198	0.0215
Accuracy (%)		NA	88.89	99.00	97.73
BW (MHz)		8	20	18	12
Q-Factor		249	112.5	76.9	94
Sensitivity (MHz/ ϵ_r)		NA	12.42	11.14	15.00

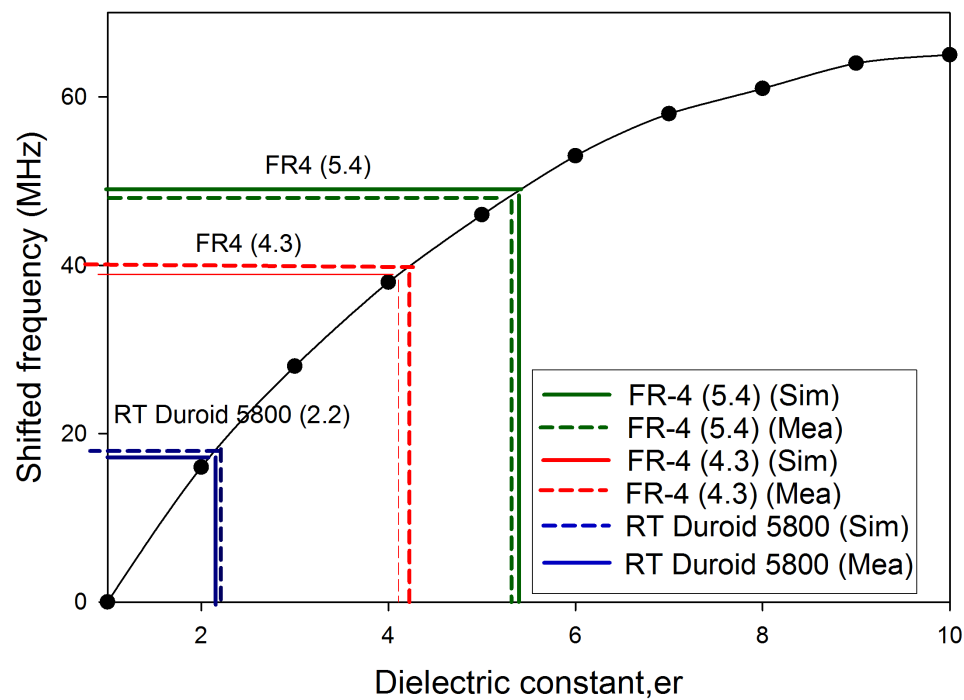


Figure 12. Material characterization measurement.

shows the accurate characterization of the sensor with the lowest accuracy of 98%. The close similarity between the simulated and actual frequency shifts indicates the sensor’s capability for precise dielectric constant characterization. The high accuracy, coupled with a low percentage error, validate the sensor’s reliability for applications requiring precise material property analysis, making it a valuable tool in advanced sensor systems. The proposed sensor demonstrates several key advantages over the sensors listed in Table 2. One notable benefit is its lower percentage error, with a value of 0.5%, which is significantly lower than the other sensors, such as [9] with 2.2%, [10] with 2.56%, and [11] with 2.68%. This reduced percentage error indicates superior accuracy, making the proposed sensor more suitable for high-precision applications. Additionally, the proposed sensor exhibits a high Q-factor of 595, surpassing the Q-factors of sensors such

as [11] with 464 and [10] with 117.5. A higher Q-factor corresponds to improved energy storage and selectivity, contributing to enhanced performance in sensing and filtering applications. While the sensitivity of the proposed sensor is relatively low at 15, this lower sensitivity can be advantageous in specific contexts where excessive sensitivity could lead to instability. In such applications, a sensor with controlled sensitivity offers greater operational stability and versatility across different conditions. Single-port microwave sensors offer several practical advantages over dual-port designs. While single-port sensors may have lower sensitivity or smaller frequency shift, they offer practical advantages in terms of simplicity, cost, and ease of use. They feature a simpler structure, requiring only one connection, which reduces hardware complexity and cost. With faster measurement times and easier calibration procedures, they are ideal for compact or embedded systems. Additionally, they minimise signal loss and are well-suited

Table 2. Comparison of proposed sensor’s performance.

Sensor	Error %	Q-factor	Sensitivity (MHz/ $\Delta\epsilon_r$)	Sensor	Type of sensors	Advantage and limitation
[9]	2.2	NR	NR	FR4	CSRR	large size
[10]	6.37	129	63	FR4	double CSRRs	High sensitivity, low Q-factor and low accuracy
[11]	9.87	357	96	RT Duroid 5800	Double CSRR-DGS	High sensitivity but expensive and low accuracy
This work	0.56	595	15	FR4	DGS	Low sensitivity but high accuracy

NR = Not Recorded

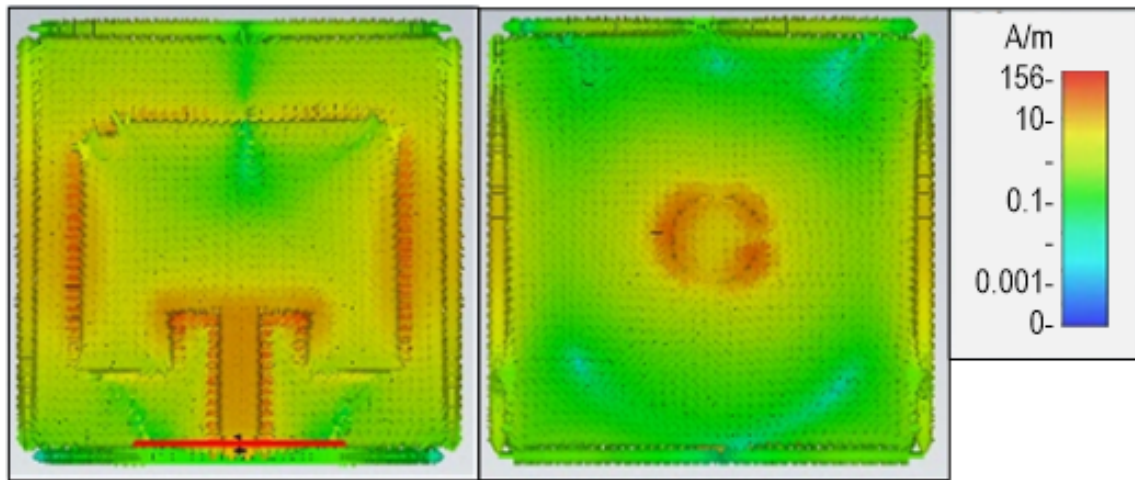


Figure 13. Surface current distribution (a) top and (b) DGS view.

for surface or non-invasive sensing applications. Surface current distribution, as shown in Fig. 13 significantly influences sensor performance in material characterization. The areas on the patch antenna with higher current intensity demonstrate stronger electromagnetic interactions with the MUT, leading to a larger frequency shift. When the MUT is placed on the patch area, higher current intensity indicates increased energy absorption, which enhances the sensitivity and accuracy of the sensor. The DGS part of the antenna exhibits high current intensity, maximizing electromagnetic interference and radiation losses. DGS enhances the accuracy of microwave sensors by concentrating the electromagnetic fields in the sensing region, thereby increasing the interaction with the MUT. When the MUT is placed near the DGS, even slight changes in its dielectric properties cause noticeable shifts in the sensor's resonant frequency. This strong field-MUT coupling results in improved sensitivity and measurement precision. Additionally, DGS helps suppress unwanted surface currents and higher-order modes, contributing to a higher Q-factor and reduced noise. As a result, the sensor exhibits sharper resonance peaks and more reliable detection, especially when characterising low-contrast or subtle material differences.

In summary, the proposed sensor offers significant advantages in terms of accuracy, performance, and cost-effectiveness, positioning it as a highly competitive option for a wide range of applications. The proposed sensor offers a novel combination of simplicity, high accuracy, and low cost, making it ideal for practical applications. Utilising a single-port design, it reduces hardware complexity, simplifies calibration, and enables faster measurements, while maintaining reliable performance, making it highly suitable for compact, efficient, and cost-effective material characterisation.

4. Conclusion

In conclusion, the proposed sensor demonstrates high accuracy, achieving a percentage error range of 0.56% to 1.86% for the tested MUT, indicating its reliability in precise measurements. The implementation of a DGS

contributes a significant role in enhancing the sensor's performance, optimizing its ability to operate efficiently while maintaining a compact design. The sensor's high Q-factor, measured at 595, allows for the detection of small changes in the dielectric constant of materials. Despite its high performance, the sensor remains cost-effective, utilizing an economical substrate while maintaining superior accuracy and selectivity. The proposed sensor is initially designed for rigid MUT, demonstrating reliable performance. To enhance its versatility, it can be further adapted for semi-solid and liquid samples, allowing broader application in material characterization. Additionally, by converting the sensor to a dual-port configuration, its sensitivity can be significantly improved, due to stronger electromagnetic field coupling and more pronounced resonance shifts in response to dielectric property variations.

Acknowledgment

The author would like to thank the Centre for Research and Innovation Management (CRIM) and Universiti Teknikal Malaysia Melaka (UTeM) for financing this work.

Authors contributions

Authors have contributed equally in preparing and writing the manuscript.

Availability of data and materials

The data that support the findings of this study are available from the corresponding author upon reasonable request.

Conflict of interests

The authors declare that they have no known competing financial interests or personal relationships that could have appeared to influence the work reported in this paper.

References

- [1] A. Armghan et al. “**Characterization of dielectric substrates using dual band microwave sensor.**”. *IEEE Access*, 9:62779–62787, 2021.
DOI: <https://doi.org/10.1109/ACCESS.2021.3075246>.
- [2] H. S. Roslan et al. “**High Sensitivity Microwave Sensor for Material Characterization Using Square Split Ring Resonator.**”. *IEEE International RF and Microwave Conference (RFM)*, pages 1–4, 2022.
DOI: <https://doi.org/10.1109/RFM56185.2022.10065034>.
- [3] S. R. Harry et al. “**Design of Dual Band Meta-Material Resonator Sensor for Material Characterization.**”. *Applied Computational Electromagnetics Society Journal*, 36(4), 2021.
DOI: <https://doi.org/10.47037/2020.ACES.J.360414>.
- [4] L. Ali et al. “**Interdigitated Planar Microwave Sensor for Characterizing Single/Multilayers Magnetodielectric Material.**”. *IEEE Microwave and Wireless Components Letters*, 32(7):619–622, 2022.
DOI: <https://doi.org/10.1109/LMWC.2022.3141129>.
- [5] X. Han et al. “**Microwave Sensor Loaded With Complementary Curved Ring Resonator for Material Permittivity Detection.**”. *IEEE Sensors Journal*, 22(19):20456–20463, 2022.
DOI: <https://doi.org/10.1109/JSEN.2022.3205639>.
- [6] C. Wang, L. Ali, F. Meng, K. K. Adhikari, Z. Zhou, Y.-C. Wei, D. Zou, and H. Yu. “**High-Accuracy Complex Permittivity Characterization of Solid Materials Using Parallel Interdigital Capacitor-Based Planar Microwave Sensor.**”. *IEEE Sensors Journal*, 21(5):6083–6093, 2021.
DOI: <https://doi.org/10.1109/JSEN.2020.3041014>.
- [7] S. Alam et al. “**High Stability Single-Port Dual Band Microwave Sensor Based on Interdigital Capacitor Structure With Asymmetry Branch Feedline.**”. *IEEE Access*, 13:24576–24586, 2025.
DOI: <https://doi.org/10.1109/ACCESS.2025.3538042>.
- [8] M. H. Misran et al. “**High Sensitivity Double Split Ring Resonator – Defected Ground Structure (DSRR-DGS) Based Microwave Sensors for Material Characterization.**”. *IEEE Asia-Pacific Conference on Applied Electromagnetics (APACE)*, Langkawi, Kedah, Malaysia, pages 440–443, 2024.
DOI: <https://doi.org/10.1109/APACE62360.2024.10877286>.
- [9] J. Oliveira, G. D. João, et al. “**CSRR-based microwave sensor for dielectric materials characterization applied to soil water content determination.**”. *Sensors*, 20(1):255, 2020.
DOI: <https://doi.org/10.3390/s20010255>.
- [10] Y. Junho and J.-I. Lee. “**Design of a high-sensitivity microstrip patch sensor antenna loaded with a defected ground structure based on a complementary split ring resonator.**”. *Sensors*, 20(24):7064, 2020.
DOI: <https://doi.org/10.3390/s20247064>.
- [11] N. Abd Rahman et al. “**High quality factor using nested complementary split ring resonator for dielectric properties of solids sample.**”. *The Applied Computational Electromagnetics Society Journal*, pages 1222–1227, 2020.